

## Synthesis and Characterization of Cobalt Oxide Nanoparticles and Cobalt Oxide/MWCNTs as a Binary Nanocomposite

S. A. Yassin<sup>(1)</sup> , H. N. Hussein<sup>(1)\*</sup> , D. A. Abdulateef<sup>(1)</sup>

<sup>(1)</sup> The General Directorate for Education of Diyala, Diyala, Iraq

### Article information

#### Article history:

Received: April 13, 2024

Revised: June 12, 2024

Accepted: June 30, 2024

Available online: September 01, 2024

#### Keywords:

Chemical Synthesis

Co<sub>3</sub>O<sub>4</sub> Nanoparticles

Multi-Walled Carbon Nanotubes

#### Correspondence:

Haider Nazar Hussein

[haiderghabee@gmail.com](mailto:haiderghabee@gmail.com)

### Abstract

There is a rising interest in nanocomposites with unanticipated features that are different from traditional materials to fulfill the demands of these applications. Cobalt oxide (Co<sub>3</sub>O<sub>4</sub>) nanoparticles, and cobalt oxide with multi-walled carbon nanotubes (Co<sub>3</sub>O<sub>4</sub>/MWCNTs) as nanocomposites were created. In this study, cobalt oxide nanoparticles (Co<sub>3</sub>O<sub>4</sub> NPs) were synthesized via co-precipitation method chemical using CoCl<sub>2</sub> salt as a source of cobalt nanoparticles and sodium hydroxide solution as a factor agent at room temperature. The cobalt hydroxide (Co(OH)<sub>2</sub>) precipitate was obtained, then it calcinated the cobalt hydroxide precipitate at 600°C to obtain the cobalt oxides nanoparticles (Co<sub>3</sub>O<sub>4</sub> NPs). Also, MWCNTs were prepared by a locally manufactured reactor at 423 K. Binary composites were prepared by solution method using cobalt oxide nanoparticles dispersion over MWCNTs surfaces. The structural, morphological, and spectral properties were confirmed and investigated by using FE-SEM, Raman spectroscopy, and (XRD), respectively. The surface area and pore size obtained by BET and BJH showed that the binary nanocomposites (Co<sub>3</sub>O<sub>4</sub>/MWCNTs) have a higher surface area than their pristine cobalt oxide and multi-walled carbon nanotubes nanoparticles. The adsorption processes of nanocomposites have attracted significant care from the scientific public because of their distinctive possessions and aptitude to reduce and adsorb Cu<sup>+2</sup> and Ni<sup>+2</sup> as heavy metals from water pollution. As a result, Co<sub>3</sub>O<sub>4</sub> and its nanocomposite with MWCNTs were used to remove copper and nickel ions from the dilute aqueous solution.

DOI: [10.33899/edusj.2024.148146.1435](https://doi.org/10.33899/edusj.2024.148146.1435), ©Authors, 2024, College of Education for Pure Science, University of Mosul.

This is an open access article under the CC BY 4.0 license (<http://creativecommons.org/licenses/by/4.0/>).

## 1. Introduction

Nanoscience has been accepted not long ago as a new interdisciplinary science. It can be defined as knowledge of fundamental properties of nanoscience objects. The ideas and concepts behind nanoscience and nanotechnology began in late 1959 with a talk entitled "There Plenty of Room at the Bottom" by physicist Richard Feynman at an American Physical Society conference, held at the California Institute of Technology in Pasadena, long before the term nanotechnology was used. Feynman described the theoretical basis of processes in which scientists would be able to manipulate and control individual atoms and molecules. [1] About ten years later Professor Norio Taniguchi at Tokyo State University coined the term nanotechnology. The nanomaterial is known as the materials that have a lower dimension in the Nano-scale range of 1–100 nm and based on the overall dimensional these materials can be 0D, 1D, 2D, or 3D [2]. NPs are not new to the environment and occur naturally in the form of minerals, clays, and products of bacteria. Engineered nanoparticles are designed to have properties that are not present in bulk samples of the same materials. [3] The variety of engineered nanomaterials is designed with different sizes and shapes to have properties that are not present in bulk samples of the same materials [4]. CoO and Co<sub>3</sub>O<sub>4</sub> are more stable than other cobalt oxides, as well as they have high stability kinetically at room temperature, hence require a lot of attention in scientific research due to their promising applications [5]. In 2004, Y. Hsiou and associates succeeded in obtaining carbon nanotubes in multiple structural configurations by different methods, this methods resulted in carbon nanotubes with lengths of 1 μm and 100 nm as diameter [6].

Materials with relatively distinct qualities, such as lightweight, chemical and mechanical resistance, thermal and electrical insulation, and design flexibility, can be combined to make nanocomposite materials, these materials do not dissolve or mix into one another, although dispersion is conceivable<sup>[7]</sup>. The unique features of the nanocomposite are a result of the interplay between its many nanoparticles <sup>[8]</sup>. Recently, carbon nanotubes have been included in composites to enhance the characteristics of polymers <sup>[9]</sup>. Al Khazraji and colleagues created MWNTs/polymer by adding 0.1 weight percent of MWCNTs and evenly dispersing them throughout the 0.3 weight percent polymer matrix <sup>[10]</sup>. The findings, which were corroborated by different physical techniques, demonstrated that MWCNT bundles were efficiently dispersed in the polymer matrix and that, when compared to carbon nanotubes without a polymer, the polymer as a matrix had a discernible impact on the diameters and longest carbon nanotube <sup>[11]</sup>. As possible electrode materials for supercapacitors, metal oxides including MnO<sub>2</sub>, ZnO, NiO, MgO, CuO, and TiO<sub>2</sub> have been explored in addition to carbon<sup>[12, 13, 14, 15]</sup>. Environmental pollution may take many different forms, including light, air, water, noise, soil, thermal, radiation, and light pollution <sup>[16]</sup>. The substances that produce environmental pollution are referred to as pollutants. The present study is focused on the synthesis of cobalt oxide nanoparticles which were used in the synthesis of Co<sub>3</sub>O<sub>4</sub>/MWCNTs as a binary nanocomposite with MWCNTs, study their characterization and adsorption of Cu<sup>+2</sup> and Ni<sup>+2</sup> ion from wastewater.

## 2. Experimental part

Analytical-grade cobalt (II) chloride hexahydrate (99%), sodium hydroxide (NaOH) (98%), and ethanol (99%) were acquired from BDH Company in England. We bought multi-walled carbon nanotubes with a diameter of 10 nm and a length of around 1.5 µm from Cheap Tube Company in the United States. Since CuSO<sub>4</sub> and NiSO<sub>4</sub> salts contain strong pollutants that need to be removed from wastewater, the heavy metals used as adsorbents in this study were Cu<sup>+2</sup> and Ni<sup>+2</sup> ions.

The samples analysis by Raman spectroscopy (Raman Tuscan 550 nm), XRD (XPERT-Pro diffractometer operating at 30 mA and 40 kV for the scanning angles from 20 to 80° is used to get the XRD pattern via irradiating the samples with Siemens model D500), FE-SEM (ZEISS model: Sigma VP are used), and BET Techniques (BET Quantachrome Nova1000e- Germany) of the prepared compounds and the study of their properties were carried out in the College of Science/University Tehran-Iran.

### 2.1. Standard Cu<sup>+2</sup> and Pb<sup>+2</sup> ion stock solution

#### 2.1.1. Sodium hydroxide

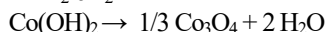
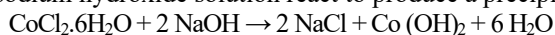
To create the (0.2) M of NaOH solution, 0.8 g of sodium hydroxide was weighed and put into a 200 mL volumetric flask. The capacity was then filled to the brim with deionized water.

#### The standard stock solution of Cu<sup>+2</sup> and Ni<sup>+2</sup> ions

Cu<sup>+2</sup> and Ni<sup>+2</sup> ions standard stock solution (1000 mg/L) CuSO<sub>4</sub> (3.979 g) and (3.5423 g) NiSO<sub>4</sub> were weighed, dissolved in deionized water, and then diluted to 1000 ml in a volumetric flask using deionized water to create the stock solution of Cu<sup>+2</sup> and Ni<sup>+2</sup> ions. A range of solutions containing 100, 150, 200, 250, and 300 mg/L were created by diluting the stock solution with deionized water in sufficient amounts.

#### 2.1.2. Preparation of Co<sub>3</sub>O<sub>4</sub> nanoparticles using chemical precipitation method.

Co<sub>3</sub>O<sub>4</sub> nanoparticles were synthesized via co-precipitation method using Cobalt (II) chloride hexahydrate (CoCl<sub>2</sub>.6H<sub>2</sub>O). A precursor salt of (1.5 g) was dissolved in 50 mL of deionized water. NaOH solution (0.1M) was slowly dropped on the salt solution under vigorous stirring until pH reached 12. The following equations describe how cobalt chloride hexahydrate solution and sodium hydroxide solution react to produce a precipitate of cobalt hydroxide:



The blue precipitate Co(OH)<sub>2</sub> was collected, and after being repeatedly cleaned with deionized water and 100% ethanol until the pH reached 7, it was dried for four hours at 80 °C. The next step is to calcine Co(OH)<sub>2</sub> for six hours at 600°C in a furnace to produce cobalt oxide nanoparticles (Co<sub>3</sub>O<sub>4</sub> NPs).

#### 2.1.3. Preparation of Co<sub>3</sub>O<sub>4</sub>/MWCNTs nanocomposite.

Using the impregnation method the Co<sub>3</sub>O<sub>4</sub>/MWCNTs as binary nanocomposites were synthesized (0.2 g of Co<sub>3</sub>O<sub>4</sub> NPs / 0.1g of MWCNTs). After suspending (0.1 g) of MWCNTs and (0.2 g) of Co<sub>3</sub>O<sub>4</sub> NPs in 30 mL of ethanol at room temperature while stirring continuously, an impregnated solution was created. The mixture was then put in a water bath apparatus. The solvent was evaporated and the nanoparticles were fully suspended after 1.5 hours, resulting in a binary nanocomposite of Co<sub>3</sub>O<sub>4</sub> and MWCNTs.

#### 2.1.4. Effect of contact time on Cu<sup>+2</sup> and Ni<sup>+2</sup> ions Adsorption

The time taken for the adsorption process to achieve equilibrium at 298 K was calculated using five volumetric flasks (100 mL) holding 50 mL of a solution containing Cu<sup>+2</sup> or Ni<sup>+2</sup> ions at an initial concentration of 100 mg/L. Each flask was filled with 0.1 g of the adsorbent (prepared Co<sub>3</sub>O<sub>4</sub> and Co<sub>3</sub>O<sub>4</sub>/MWCNTs), sealed with a glass stopper, and put in a water bath shaker set at a constant temperature of 298 K and 200 rpm for a range of time intervals (20, 40, 60, 80, and 100 min). After filtering the solutions to remove interference from Co<sub>3</sub>O<sub>4</sub> and Co<sub>3</sub>O<sub>4</sub>/MWCNT nanoparticles, the concentrations of Cu<sup>+2</sup> or Ni<sup>+2</sup> ions in the solutions

were measured using an atomic absorption spectrophotometer to attain equilibrium. The  $\lambda_{\text{max}}$  of the  $\text{Cu}^{+2}$  and  $\text{Ni}^{+2}$  ions were found to be (324.7) nm and (232.0) nm, respectively.

#### 2.1.5. Effect of quantity of $\text{Co}_3\text{O}_4$ and $\text{Co}_3\text{O}_4/\text{MWCNTs}$ as adsorbent

For the removal of  $\text{Cu}^{+2}$  or  $\text{Ni}^{+2}$  ions, the impact of the adsorbent amount was investigated using (0.2, 0.4, 0.6, 0.8, and 1) g from (prepared  $\text{Co}_3\text{O}_4$  and  $\text{Co}_3\text{O}_4/\text{MWCNTs}$ ), at a temperature of (298) K and a swirling speed of (200) rpm. The fixed (50) mL of (100) mg/L  $\text{Cu}^{+2}$  or  $\text{Ni}^{+2}$  ions was used. In every instance, the adsorption contact time was 60 minutes.

### 3. Results And Discussion

#### 3.1. Raman spectroscopy

Raman spectra of MWCNTs and their binary nanocomposite ( $\text{Co}_3\text{O}_4/\text{MWCNTs}$ ) are presented in Figure 1(A and B) respectively. There are two peaks in the MWCNTs structure observed. In the  $\text{Co}_3\text{O}_4/\text{MWCNTs}$  nanocomposite, the D band was seen at  $1436\text{ cm}^{-1}$  and the G band at  $1582\text{ cm}^{-1}$ .<sup>[17]</sup> The D band corresponds to the degree of nanotube structural disorder and the G band to the degree of graphitization of nanotubes. These measurements were made at  $1352\text{ cm}^{-1}$  and  $1580\text{ cm}^{-1}$ , respectively. Furthermore, the 2D band was identified, which corresponds to tensions at  $2932\text{ cm}^{-1}$ .<sup>[18]</sup> in the case of MWCNTs, while disappearance in the  $\text{Co}_3\text{O}_4/\text{MWCNTs}$  nanocomposite.

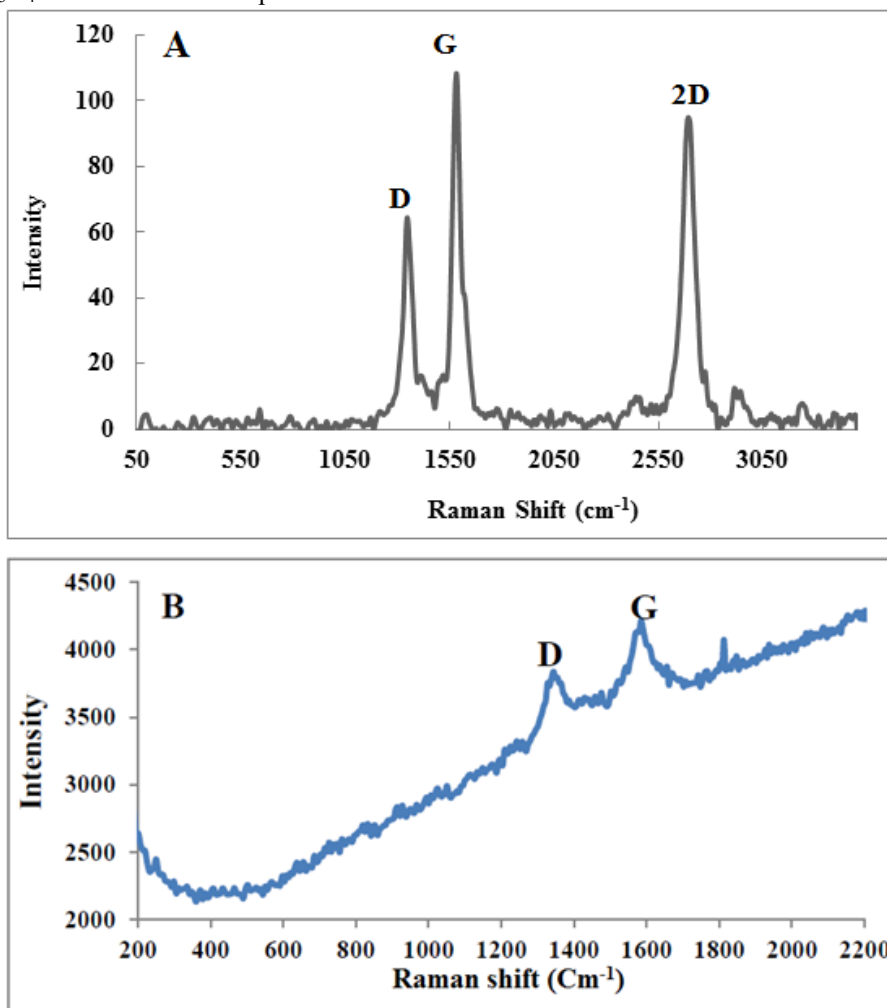


**Figure1.** Raman spectra of (A) MWCNTs and  $\text{Co}_3\text{O}_4/\text{MWCNTs}$  nanocomposite.

#### 3.2. Structural Properties

The XRD pattern of  $\text{Co}_3\text{O}_4$  NPs is seen in Figure 2. The planes (111), (220), (311), (222), (400), (422), (333), and (440) are associated with all of the strong and sharp diffraction peaks at  $2\theta$  values 19.13, 31.40, 37.00, 38.71, 44.95, 55.81, 59.50, and 65.36. These values are in good agreement with the standard XRD data for the cubic phase of  $\text{Co}_3\text{O}_4$  (JPPDS no.00-900-5887).

$\text{Co}_3\text{O}_4$  NPs' average particle size was determined using the Debye–Scherer formula. It is discovered that the lattice parameter ( $a=b=c$ ) and the average particle size are 8.0821 Å and 35.91 nm, respectively. As can be seen in Figure (2), the XRD results for the product MWCNTs that were synthesized indicate that just two peak point values  $37.07^\circ$  and  $45.5^\circ$  were obtained for the prepared sample. This indicates that the MWCNTs that were purchased are crystalline and composed of tubes with a diameter of 10.6 nm<sup>[19]</sup>. This peak value indicates that carbon is present in the product. On the other hand, the dispersion of cobalt oxide nanoparticles over and interface multi-walled carbon nanotubes (MWCNTs) surface for binary nanocomposite formation is clear, through the destruction of the cobalt oxide and MWCNTs peaks, and this is evidence and confirmed of good interference and dispersion of cobalt oxide nanoparticles in the MWCNTs as shown in Figure 2.

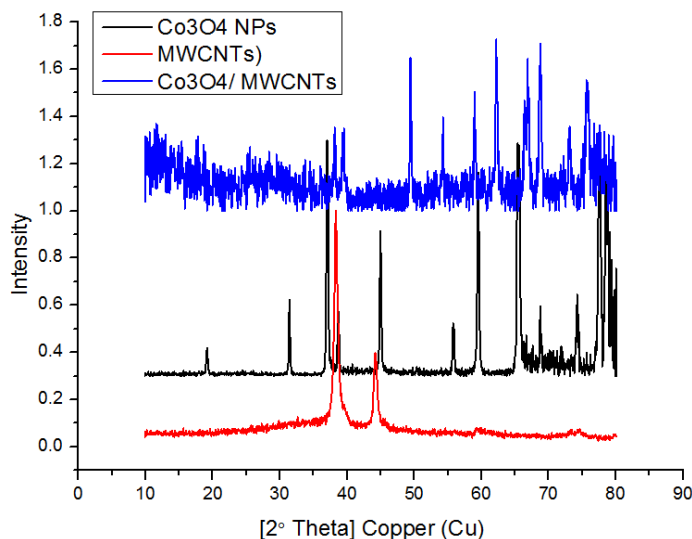


**Figure2.** XRD pattern of  $\text{Co}_3\text{O}_4$  NPs, MWCNTs and  $\text{Co}_3\text{O}_4$ / MWCNTs prepared XRD of MWCNTs.

### 3.3. FE-SEM images

Surface morphology for the prepared  $\text{Co}_3\text{O}_4$  nanoparticle is studied using the FE-SEM technique. Figure 3 shows the FE-SEM image of prepared  $\text{Co}_3\text{O}_4$  nanoparticles. It shows that the particles are in almost irregular shape and conglomerates some structures like islands are obtained. The close analysis of the diameter of the islands gave an average size of nanoparticles is 208 nm.

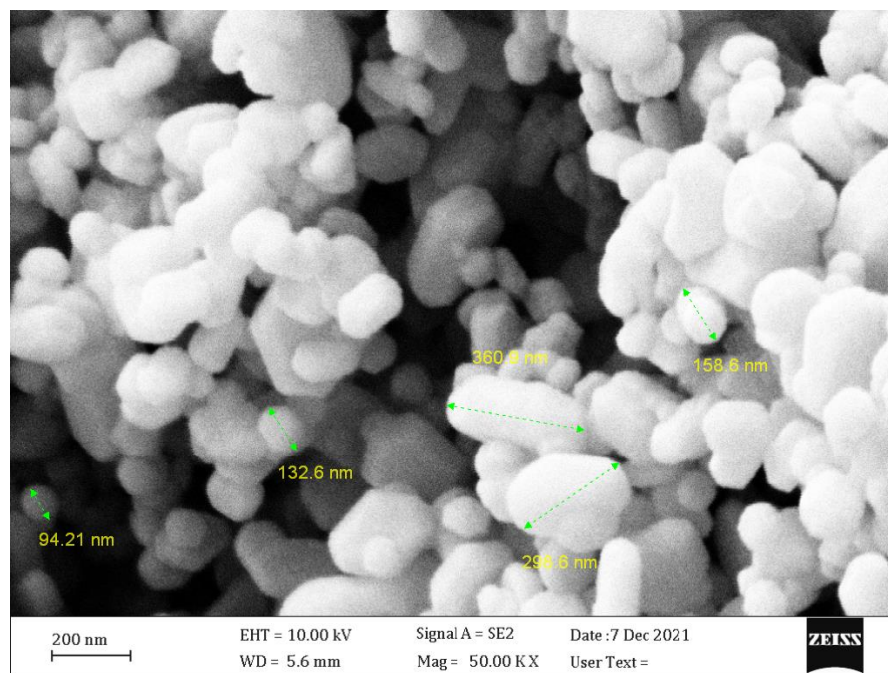


**Figure. 3.** FE-SEM micrograph of  $\text{Co}_3\text{O}_4$  nanoparticles.

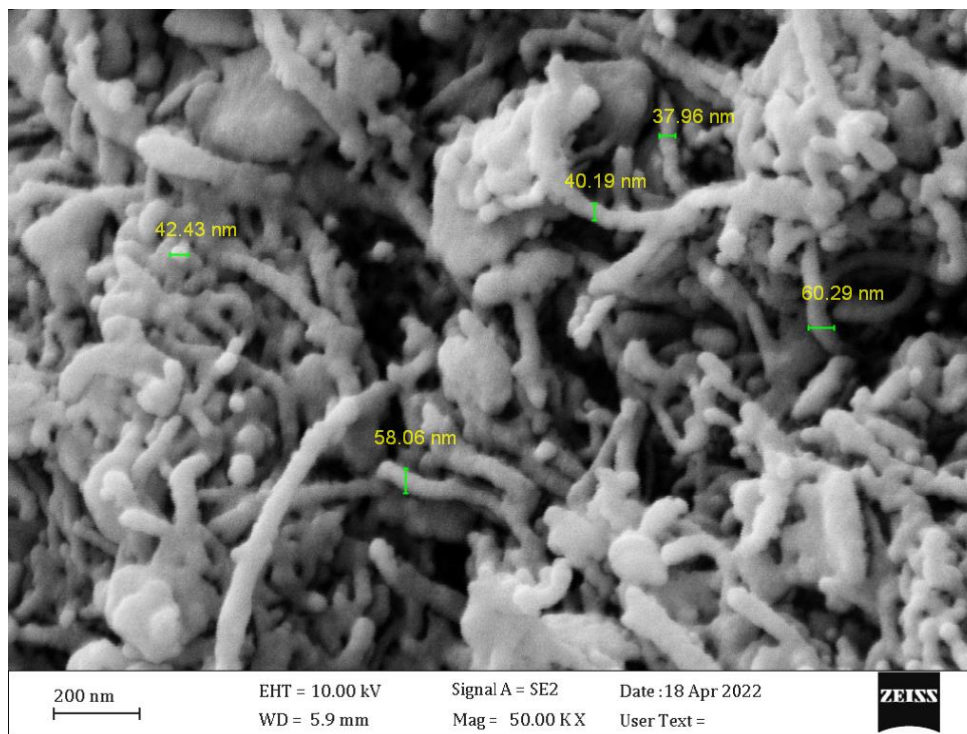


**Figure 4.** FE-SEM micrograph of MWCNTs.

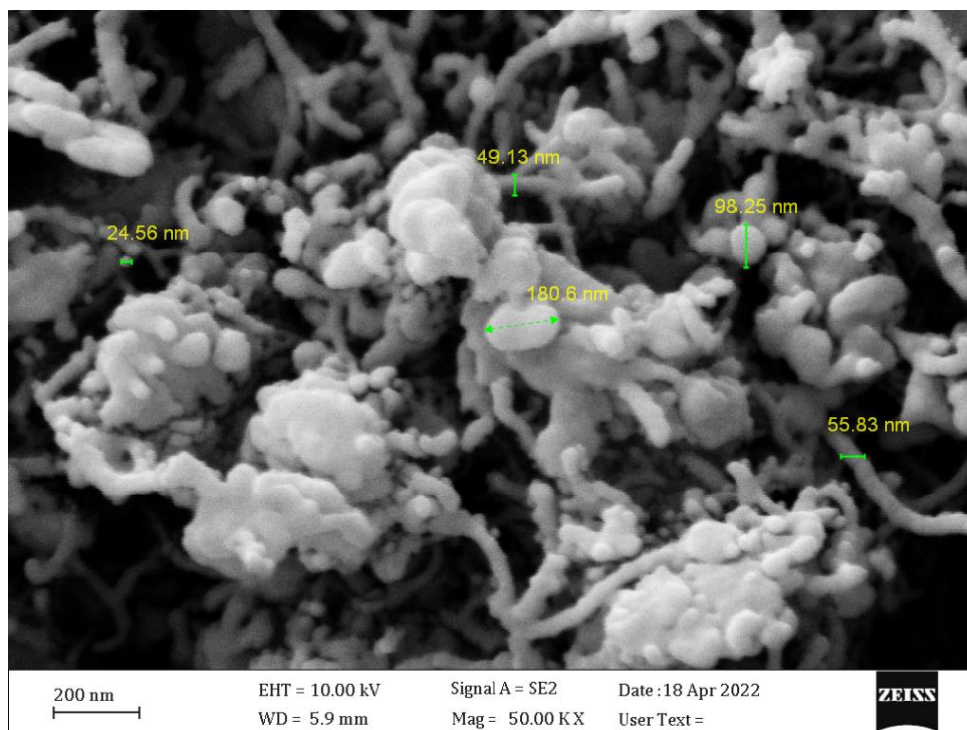


**Figure 5.** FE-SEM micrograph of  $\text{Co}_3\text{O}_4$  /MWCNTs nanocomposite.



A small number of carbon filaments with an average diameter of 47.4 nm and a length of more than 1  $\mu\text{m}$ , together with several species of unconverted carbon, are visible in the FE-SEM picture (Fig. 4) of the MWCNTs. Furthermore, as seen in Figure 4, the outside surface of the pristine MWCNTs' tubes was smooth, but the outer surface of the binary nanocomposite's ( $\text{Co}_3\text{O}_4/\text{MWCNTs}$ ) tubes was rough and included some disfigurements. Furthermore, the pristine MWCNTs' diameter was less than that of the  $\text{Co}_3\text{O}_4/\text{MWCNTs}$ , which was 81.2 nm. The dispersion technique used to create the nanocomposite synthesis caused damage to some of the MWCNT tubes' outer surfaces, which resulted in some of the tubes' outer layers becoming deformed. Comparing Figure 4 with Figure 5 shows damaged filament of carbon and they clearly show that most of the synthesized carbon nanotubes look completely covered with  $\text{Co}_3\text{O}_4$  nanoparticles. The reason behind the spread of the synthesized  $\text{Co}_3\text{O}_4$  nanoparticles might be due to the fact that they have their spread within the matrix structure and this is the common characteristic for all matrixes with carbon nanotubes. [20]

### 3.4. BET analysis

The surface area of the  $\text{Co}_3\text{O}_4$  NPs and  $\text{Co}_3\text{O}_4/\text{MWCNTs}$  nanocomposite were calculated by BET analysis technique, the surface area is  $24.123 \text{ m}^2/\text{g}$  with an average pore diameter is 36.082 nm, and the total pore volume of about  $0.1824 \text{ cm}^3/\text{g}$  for  $\text{Co}_3\text{O}_4/\text{MWCNTs}$  nanocomposite, in addition to, BJH analysis shown the presence of mesopores (pores 2–45 nm in diameter). While the BET surface area of the  $\text{Co}_3\text{O}_4$  was calculated to give a surface area of about  $16.049 \text{ m}^2/\text{g}$  with an average pore diameter of 47.363 nm and total pore volume of  $0.1638 \text{ cm}^3/\text{g}$ , BJH analyses gave mesopores (pores 2–48 nm in diameter).

### 3.5. Effect of contact time on adsorption

The study examined the impact of contact duration on the adsorption of  $\text{Cu}^{+2}$  and  $\text{Ni}^{+2}$  ions on (synthesized  $\text{Co}_3\text{O}_4$  and  $\text{Co}_3\text{O}_4/\text{MWCNTs}$ ) at concentrations of (100) mg/L of each metal ion for 20, 40, 60, 80, and 100 minutes at 298 degrees Celsius. The % removal of  $\text{Cu}^{+2}$  and  $\text{Ni}^{+2}$  ions changes with contact time, as shown in Tables (1) and (2), respectively. They demonstrate that the equilibrium time needed for both ions to adsorb on the  $\text{Co}_3\text{O}_4$  and  $\text{Co}_3\text{O}_4/\text{MWCNTs}$  is about sixty minutes. The effects of contact time on the adsorption of  $\text{Cu}^{+2}$  and  $\text{Ni}^{+2}$  ions on ( $\text{Co}_3\text{O}_4$  and  $\text{Co}_3\text{O}_4/\text{MWCNTs}$ ) surfaces are also explained in figures (6) and (7), which show a gradual increase in the percentage removal of  $\text{Cu}^{+2}$  and  $\text{Ni}^{+2}$  ions for surfaces after a decrease in the percent removal at the beginning of contact time with both ions. This could be because the adsorbent's excess adsorption sites are responsible for the rapid initial rate increase followed by a slow rate at a later period. [21] The initial high adsorption rate may have resulted from ion exchange, which was followed by a gradual chemical process involving the metal ions' active groups on the sample. Repulsive force makes it difficult for the remaining unoccupied surface sites to be occupied. [22] The metal ions must go through the pores farther and deeper, coming up against more resistance.

**Table 1: At 298 K, the adsorption of  $\text{Cu}^{+2}$  and  $\text{Ni}^{+2}$  ions by  $\text{Co}_3\text{O}_4$  NPs is affected by contact time.**

Time, min	$\text{Cu}^{+2}$			$\text{Ni}^{+2}$	
	$\text{C}_0$ , mg/L	$\text{C}_t$ , mg/L	% Removal	$\text{C}_t$ , mg/L	% Removal
20	100	20.34	79.66	18.14	81.86
40	100	16.71	83.29	17.29	82.71
60	100	14.03	85.97	15.05	84.95
80	100	13.13	86.87	12.74	87.26
100	100	12.53	87.47	11.01	88.99

**Table 2: At 298 K, the adsorption of  $\text{Cu}^{+2}$  and  $\text{Ni}^{+2}$  ions by  $\text{Co}_3\text{O}_4/\text{MWCNTs}$  nanocomposite is affected by contact time.**

Time, min	$\text{Cu}^{+2}$			$\text{Ni}^{+2}$	
	$\text{C}_0$ , mg/L	$\text{C}_t$ , mg/L	% Removal	$\text{C}_t$ , mg/L	% Removal
20	100	17.09	82.91	21.06	78.94
40	100	15.41	84.59	19.61	80.39
60	100	12.11	87.89	17.05	82.95
80	100	9.54	90.46	15.23	84.77
100	100	7.29	92.71	12.38	87.62

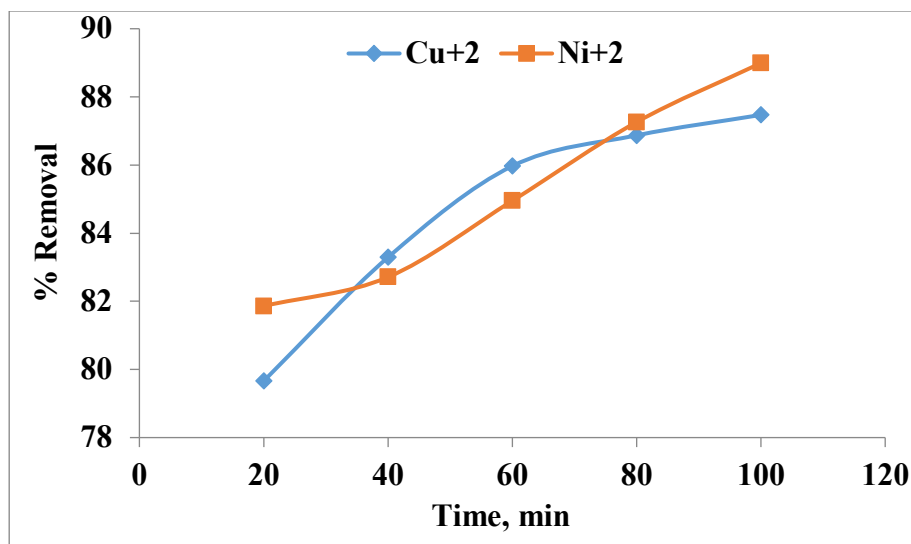


Figure 5. Effect of contact time on removal (%) of Cu<sup>2+</sup> and Ni<sup>2+</sup> ions on Co<sub>3</sub>O<sub>4</sub> NPs at 298 K.

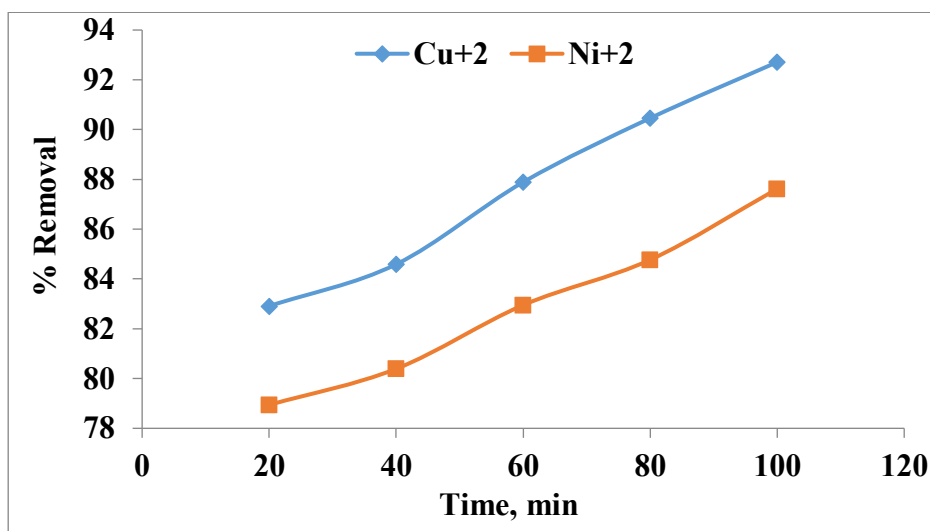


Figure 6. Effect of contact time on removal (%) of Cu<sup>2+</sup> and Ni<sup>2+</sup> ions on Co<sub>3</sub>O<sub>4</sub>/MWCNTs at 298 K.

### 3.6. Effect of adsorbent quantity on adsorption

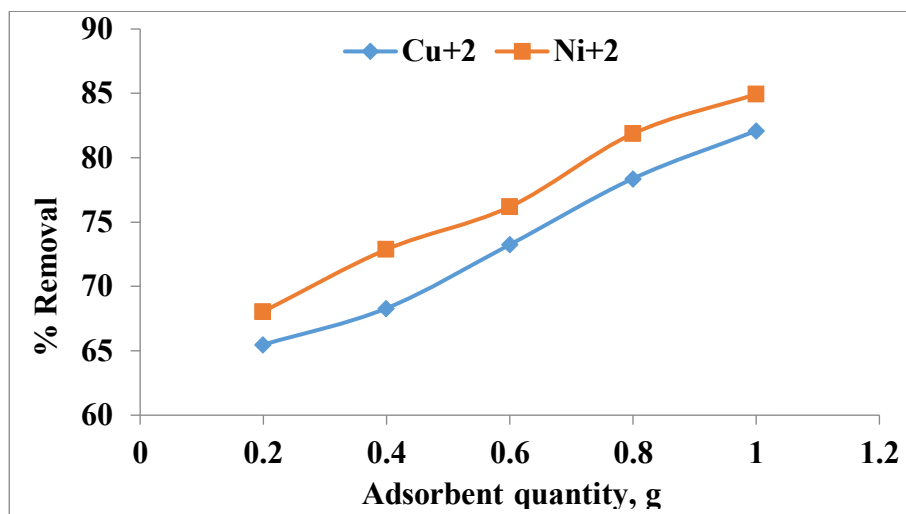
The impact of varying adsorbent quantities (0.2, 0.4, 0.6, 0.8, and 1) g at (298) K, a fixed concentration of Cu<sup>2+</sup> and Ni<sup>2+</sup> ions (100) mg/L, and a contact time (100) min for both ions were used to study the effect of adsorbent quantity on the surfaces of (Co<sub>3</sub>O<sub>4</sub> and Co<sub>3</sub>O<sub>4</sub>/MWCNTs). Tables (3) and (4) as well as Figures (7) and (8) illustrate how the quantity of adsorbent affects the uptake of Cu<sup>2+</sup> and Ni<sup>2+</sup> ions onto Co<sub>3</sub>O<sub>4</sub> and Co<sub>3</sub>O<sub>4</sub>/MWCNTs. As the quantity of Co<sub>3</sub>O<sub>4</sub> and Co<sub>3</sub>O<sub>4</sub>/MWCNTs increases, so does the removal of the metal; this implies that the percentage of metals removed increases as the amount of oxide nanoparticles increases due to increasing in the surface area.<sup>[22]</sup>

Table 3: At 298 K and 60 min, the adsorption of Cu<sup>2+</sup> and Ni<sup>2+</sup> ions by Co<sub>3</sub>O<sub>4</sub> NPs is affected by adsorbent quantity.

adsorbent quantity, g	C <sub>0</sub> , mg/L	Cu <sup>2+</sup>		Ni <sup>2+</sup>	
		Ct, mg/L	% Removal	Ct, mg/L	% Removal
0.2	100	34.52	65.48	31.94	68.06
0.4	100	31.69	68.31	27.12	72.88
0.6	100	26.75	73.25	23.81	76.19
0.8	100	21.62	78.38	18.13	81.87
1	100	17.91	82.09	15.06	84.94

**Table 3: At 298 K and 60 min, the adsorption of  $\text{Cu}^{+2}$  and  $\text{Ni}^{+2}$  ions by  $\text{Co}_3\text{O}_4/\text{MWCNTs}$  nanocomposite is affected by adsorbent quantity.**

adsorbent quantity, g	$\text{C}_0$ , mg/L	$\text{Cu}^{+2}$		$\text{Ni}^{+2}$	
		Ct, mg/L	% Removal	Ct, mg/L	% Removal
0.2	100	29.05	70.95	26.98	73.02
0.4	100	25.26	74.74	23.57	76.43
0.6	100	17.14	82.86	16.14	83.86
0.8	100	13.22	86.78	12.08	87.92
1	100	9.17	90.83	8.67	91.33



**Figure 7.** Effect of adsorbent quantity on removal (%) of  $\text{Cu}^{+2}$  and  $\text{Ni}^{+2}$  ions on  $\text{Co}_3\text{O}_4$  NPs at 298 K and 60 min.

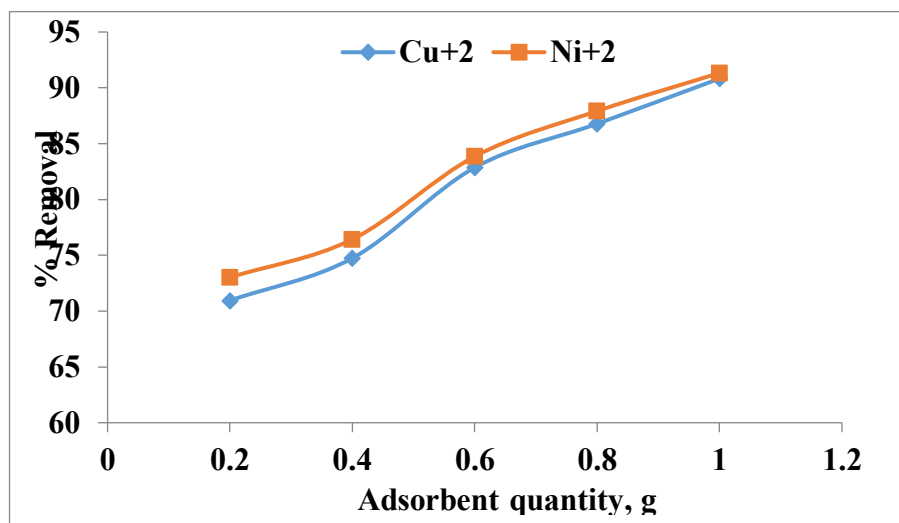


**Figure 8.** Effect of adsorbent quantity on removal (%) of  $\text{Cu}^{+2}$  and  $\text{Ni}^{+2}$  ions on  $\text{Co}_3\text{O}_4/\text{MWCNTs}$  at 298 K and 60 min

#### 4. Conclusion

co-precipitation method was successfully used for  $\text{Co}_3\text{O}_4$  nanoparticle production, and by impregnation method, the  $\text{Co}_3\text{O}_4/\text{MWCNTs}$  were successfully synthesized. Raman spectroscopy revealed D and G bands present as evidence for the MWCNTs and  $\text{Co}_3\text{O}_4/\text{MWCNTs}$ , with the ratio of ID/IG of the pristine MWCNTs (0.85) being less than activated MWCNTs (0.9). XRD revealed  $\text{Co}_3\text{O}_4$  nanoparticle synthesis with average particle size and the lattice parameter ( $a=b=c$ ) are 35.91 nm and 8.0821 Å respectively. The FE-SEM image of the  $\text{Co}_3\text{O}_4$  nanoparticles was almost irregular in shape and conglomerates some



structures like islands were obtained with an average size diameter of 208 nm, while if comparing the FE-SEM image of the  $\text{Co}_3\text{O}_4$  with the FE-SEM image of the  $\text{Co}_3\text{O}_4/\text{MWCNTs}$ , shows damage filament of carbon and they clearly show that most of the synthesized carbon nanotubes look completely covered with  $\text{Co}_3\text{O}_4$  nanoparticles, this due to behind the good dispersion of the  $\text{Co}_3\text{O}_4$  nanoparticles within the matrix structure (MWCNTs). The percentage removal of  $\text{Cu}^{+2}$  and  $\text{Ni}^{+2}$  ions reaches equilibrium in contact time (100) min and adsorbent quantity (1 g) for  $\text{Co}_3\text{O}_4$  and  $\text{Co}_3\text{O}_4/\text{MWCNTs}$ .

## 5. Acknowledgments

First, we want to give our thanks to the General Directorate for Education of Diyala, we are very grateful and render thanks to our colleagues for helping to complete this research.

## 6. References

- [1] Bayda, S.; Adeel, M.; Tuccinardi, T.; Cordani, M.; Rizzolio, F., The history of nanoscience and nanotechnology: from chemical–physical applications to nanomedicine. *Molecules* **2019**, *25* (1), 112.
- [2] Mekuye, B.; Abera, B., Nanomaterials: An overview of synthesis, classification, characterization, and applications. *Nano Select* **2023**, *4* (8), 486-501.
- [3] Bandala, E. R.; Berli, M., Engineered nanomaterials (ENMs) and their role at the nexus of Food, Energy, and Water. *Materials Science for Energy Technologies* **2019**, *2* (1), 29-40.
- [4] Barhoum, A.; García-Betancourt, M. L.; Jeevanandam, J.; Hussien, E. A.; Mekkawy, S. A.; Mostafa, M.; Omran, M. M.; S. Abdalla, M.; Bechelany, M., Review on natural, incidental, bioinspired, and engineered nanomaterials: history, definitions, classifications, synthesis, properties, market, toxicities, risks, and regulations. *Nanomaterials* **2022**, *12* (2), 177.
- [5] Gazulla, M. F.; Ventura, M.; Andreu, C.; Gilabert, J.; Orduna, M.; Rodrigo, M., Characterization of cobalt oxides transformations with temperature at different atmospheres. *Int J Chem Sci Res* **2019**, *17*, 312.
- [6] Rathinavel, S.; Priyadharshini, K.; Panda, D., A review on carbon nanotube: An overview of synthesis, properties, functionalization, characterization, and the application. *Materials Science and Engineering: B* **2021**, *268*, 115095.
- [7] Chen, J.; Wei, S.; Xie, H. In *A brief introduction of carbon nanotubes: history, synthesis, and properties*, Journal of Physics: Conference Series, IOP Publishing: 2021; p 012184.
- [8] Sen, M., Nanocomposite materials. *Nanotechnology and the Environment* **2020**, 1-12.
- [9] Gado, W. S.; Aboalkhair, M.; Al-Gamal, A.; Kabel, K. I., New Trends and Challenges of Smart Sensors Based on Polymer Nanocomposites. **2024**.
- [10] Munther, A.; Al Khazraji, A. H.; Katan, M., Multi-Walled Carbon Nanotubes (MWCNT) Dispersion over Novel Polymer Matrix. *Solid State Technology* **2020**, *63* (5), 3554-3565.
- [11] Rennhofer, H.; Zanghellini, B., Dispersion State and Damage of Carbon Nanotubes and Carbon Nanofibers by Ultrasonic Dispersion: A Review. *Nanomaterials* **2021**, *11*, 1469. **2021**.
- [12] Pant, B.; Park, M.; Park, S.-J.,  $\text{TiO}_2$  NPs assembled into a carbon nanofiber composite electrode by a one-step electrospinning process for supercapacitor applications. *Polymers* **2019**, *11* (5), 899.
- [13] Wu, D.; Xie, X.; Zhang, Y.; Zhang, D.; Du, W.; Zhang, X.; Wang, B.,  $\text{MnO}_2/\text{carbon}$  composites for supercapacitor: synthesis and electrochemical performance. *Frontiers in Materials* **2020**, *7*, 2.
- [14] Guo, G.; Zhou, Z.; Li, J.; Yan, H.; Li, F., Preparation of lignin carbon/zinc oxide electrode material and its application in supercapacitors. *Molecules* **2021**, *26* (12), 3554.

- [15]Wang, R.; Li, X.; Nie, Z.; Zhao, Y.; Wang, H., Metal/metal oxide nanoparticles-composited porous carbon for high-performance supercapacitors. *Journal of Energy Storage* **2021**, 38, 102479.
- [16]Ali, R.; Rawlins, T., Investigations: Environmental Pollution Dumping. *Encyclopedia of Security and Emergency Management* **2021**, 548-553.
- [17]Yassin, S. A.; Al Khazraji, A. H.; Abdulrazzak, F. H. In *Synthesis of carbon nanotubes by the catalytic flame deposition of coal*, AIP Conference Proceedings, AIP Publishing: 2020.
- [18]Mohan, S.; Oluwafemi, O. S.; Songca, S. P.; Rouxel, D.; Miska, P.; Lewu, F. B.; Kalarikkal, N.; Thomas, S., Completely green synthesis of silver nanoparticle decorated MWCNT and its antibacterial and catalytic properties. *Pure and Applied Chemistry* **2016**, 88 (1-2), 71-81.
- [19]Soleimani, H.; Baig, M. K.; Yahya, N.; Khodapanah, L.; Sabet, M.; Demiral, B. M.; Burda, M., Impact of carbon nanotubes based nanofluid on oil recovery efficiency using core flooding. *Results in Physics* **2018**, 9, 39-48.
- [20]Mallakpour, S.; Khadem, E., Carbon nanotube–metal oxide nanocomposites: Fabrication, properties and applications. *Chemical Engineering Journal* **2016**, 302, 344-367.
- [21]De Gisi, S.; Lofrano, G.; Grassi, M.; Notarnicola, M., Characteristics and adsorption capacities of low-cost sorbents for wastewater treatment: A review. *Sustainable Materials and Technologies* **2016**, 9, 10-40.
- [22]El Mouden, A.; El Messaoudi, N.; El Guerra, A.; Bouich, A.; Mehmeti, V.; Lacherai, A.; Jada, A.; Sher, F., Multifunctional cobalt oxide nanocomposites for efficient removal of heavy metals from aqueous solutions. *Chemosphere* **2023**, 317, 137922.

## تحضير وتشخيص الجسيمات النانوية لأوكسيد الكوبالت وأكسيد الكوبالت/أنابيب الكربون النانوية متعددة الجدران كمترابك ثنائي نانوي

صفا احمد ياسين<sup>1</sup>, حيدر نزار حسين<sup>1</sup>, دنيا احمد عبد اللطيف<sup>1</sup>

<sup>1</sup>مديرية تربية ديالى, ديالى, العراق

### المستخلص

هناك اهتمام متزايد بالمركبات النانوية ذات الميزات غير المتوقعة التي تختلف عن المواد التقليدية لتلبية متطلبات هذه التطبيقات. تم إنشاء جزيئات أكسيد الكوبالت ( $\text{Co}_3\text{O}_4$ ) النانوية، وأكسيد الكوبالت مع أنابيب الكربون النانوية متعددة الجدران ( $\text{Co}_3\text{O}_4/\text{MWCNTs}$ ) كمركبات نانوية. في هذه الدراسة، تم تصنيع جسيمات أكسيد الكوبالت النانوية ( $\text{Co}_3\text{O}_4$  NPs) بطريقة الترسيب المشترك الكيميائية باستخدام ملح  $\text{CoCl}_2$  كمصدر لجسيمات الكوبالت النانوية ومحلول هيدروكسيد الصوديوم كعامل ترسيب عند درجة حرارة الغرفة. تم الحصول على راسب هيدروكسيد الكوبالت ( $\text{Co}(\text{OH})_2$ ) ثم تكلس راسب هيدروكسيد الكوبالت عند درجة حرارة 600 درجة مئوية للحصول على جزيئات أكسيد الكوبالت النانوية ( $\text{Co}_3\text{O}_4$  NPs). كما تم تحضير MWCNTs بواسطة مفاعل مصنع محلياً بطاقة 423 k. تم تحضير المركب الثنائي بطريقة الحل باستخدام تشتت جزيئات أكسيد الكوبالت النانوية على أسطح MWCNT. تم التحقق من الخصائص التركيبية، المورفولوجية، والطيفية باستخدام FE-SEM، مطيافية رامان، و (XRD) على التوالي. تم الحصول على مساحة السطح وحجم المسام بواسطة BET و BJH، وأظهر أن المركبات النانوية الثنائية ( $\text{Co}_3\text{O}_4/\text{MWCNTs}$ ) لها مساحة سطح أعلى من تلك الأصلية المكونة من أكسيد الكوبالت والجسيمات النانوية لأنابيب الكربون النانوية متعددة الجدران. لقد اجتذبت عمليات الامتزاز للمركبات النانوية اهتماماً كبيراً في المجتمع العلمي بسبب خصائصها المميزة وقدرتها على تقليل وامتصاص  $\text{Cu}^{+2}$  و  $\text{Ni}^{+2}$  كمعادن ثقيلة من تلوث المياه. ونتيجة لذلك، تم استخدام  $\text{Co}_3\text{O}_4$  ومركبته النانوية مع MWCNTs لإزالة أيونات النحاس والنيكل من المحلول المائي المخفف.